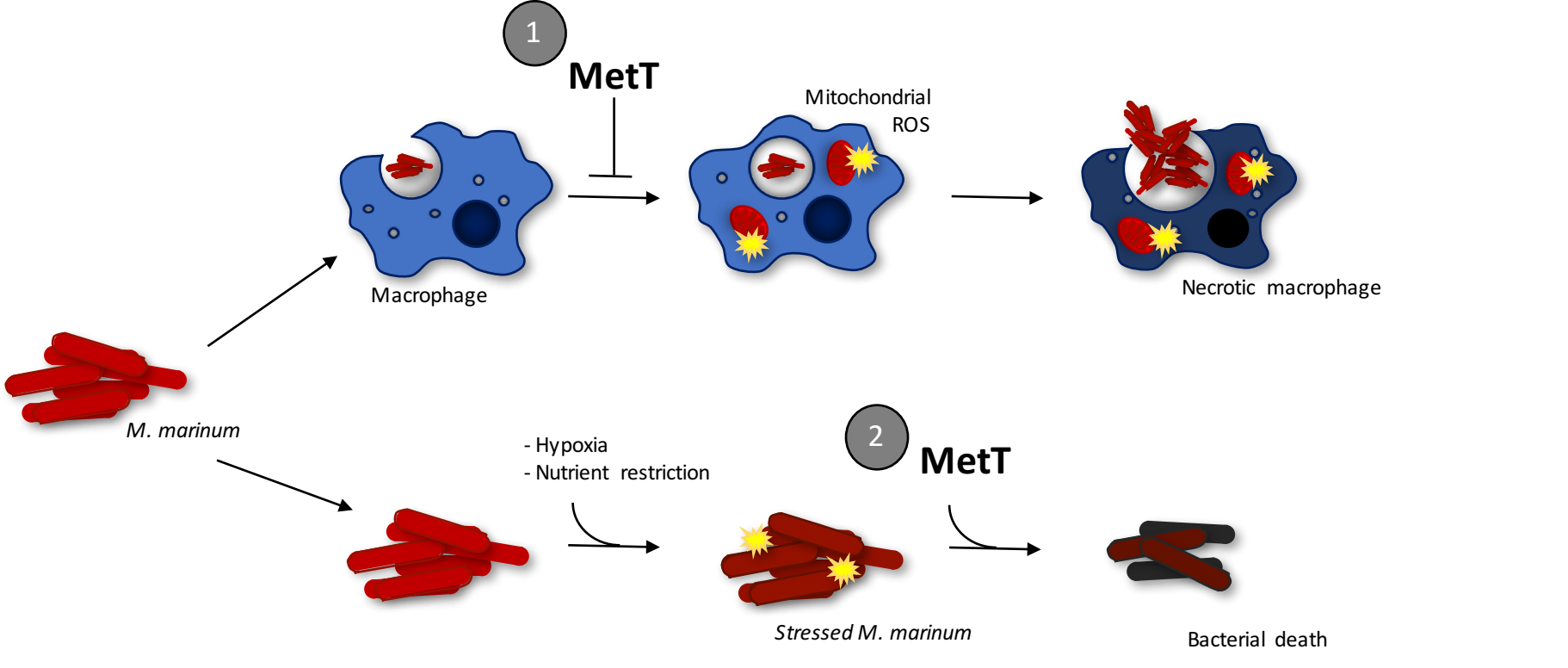
1
MetT
Mitochondrial
ROS
Macrophage
Necrotic macrophage
M. marinum
- Hypoxia
- Nutrient restriction
2
MetT
Stressed M. marinum
Bacterial death

This accepted manuscript has been published in Free Radical Biology and Medicine
https://doi.org/10.1016/j.freeradbiomed.2019.03.010

The cyclic nitroxide antioxidant 4-methoxy-TEMPO decreases mycobacterial burden *in vivo* through host and bacterial targets

Harrison D Black[a,b], Wenbo Xu[a], Elinor Hortle[a,c], Sonia I Roberston[a], Warwick J Britton[a,c], Amandeep Kaur[d], Elizabeth J New[d], Paul K Witting[b], Belal Chami[b], Stefan H Oehlers[a,c]*

[a] Centenary Institute, The University of Sydney, Australia.

[b] The University of Sydney, Discipline of Pathology Faculty of Medicine and Health, Australia.

[c] The University of Sydney, Central Clinical School Faculty of Medicine and Health and Marie Bashir Institute, Australia.

[d] The University of Sydney, School of Chemistry, Australia.

* Corresponding author, email address: stefan.oehlers@sydney.edu.au, postal address: Locked Bag 6, Newtown NSW Australia, telephone +6129565612, twitter @oehlerslab

Abstract

Tuberculosis is a chronic inflammatory disease caused by persistent infection with *Mycobacterium tuberculosis*. The rise of antibiotic resistant strains necessitates the design of novel treatments. Recent evidence shows that not only is *M. tuberculosis* highly resistant to oxidative killing, it also co-opts host oxidant production to induce phagocyte death facilitating bacterial dissemination. We have targeted this redox environment with the cyclic nitroxide derivative 4-methoxy-TEMPO (MetT) in the zebrafish-*M. marinum* infection model. MetT inhibited the production of mitochondrial ROS and decreased infection-induced cell death to aid containment of infection. We identify a second mechanism of action whereby stress conditions, including hypoxia, found in the infection microenvironment appear to sensitise *M. marinum* to killing by MetT both *in vitro* and *in vivo*. Together, our study demonstrates MetT inhibited the growth and dissemination of *M. marinum* through host and bacterial targets.

Key words

Infection; host-directed therapy; antioxidant; mitochondria; cell death, hypoxia, zebrafish

1. Introduction

Tuberculosis (TB) is a communicable disease of global health concern. TB is caused by persistent infection with *Mycobacteria tuberculosis (Mtb)*, an intracellular bacterial pathogen that can evade the immune response and persist in even immunocompetent patients for life. The prevalence of antibiotic resistance in circulating *Mtb* strains is rising, highlighting the need for novel anti-infective and host tissue-sparing strategies [1].

The pathogenesis of *Mtb* infection is a function of the complex interaction between the virulence of *Mtb* and the host immune response [2]. Within macrophages, *Mtb* faces many mechanisms of killing including lysosomal acidification of the phagosome and oxidative killing [3]. Cytokine signalling from IL-1β and TNFα, and pattern recognition signalling induce the expression of phagocytic NADPH oxidase (NOX) and inducible nitric oxide synthase (iNOS) in mycobacteria-infected macrophages [3, 4]. Phagocyte activation is required for the production of key microbicidal reactive oxygen species (ROS) including superoxide ions (O_2^-), hydrogen peroxide (H_2O_2), and hydroxyl radicals (•OH). ROS are highly effective microbicidal molecules, but pathogenic mycobacteria are highly resistant to oxidative mediated killing through expression of catalase, superoxide dismutase, and peroxiredoxin enzymes that detoxify ROS to benign products [3].

Inflammation stimulates expression of NOX and NOS, and the production of ROS in the mitochondria [5]. Disruption of the tightly regulated balance between oxidants and antioxidants results in pathological oxidation of proteins, lipids, and nucleic acid causing

oxidative stress and cell death [6]. Evidence suggests that pathogenic mycobacteria co-opt the host immune response to facilitate a growth-permissive environment, through the modulation of host oxidant production. Roca and Ramakrishnan showed that mitochondrial superoxide was upregulated during mycobacterial infection caused by signalling from TNF through the RIP1/RIP3 pathway favouring necroptotic cell death and the detrimental release of intracellular mycobacteria [7]. Further, they demonstrated oxidant scavenging molecules, including the cyclic nitroxide TEMPOL, were able to inhibit the growth of mycobacteria and cell death in conditions of TNF overexpression but not in wild type animals [7].

Dallenga *et al.* also demonstrated that host oxidant production benefited pathogen replication using an *in vitro* macrophage and neutrophil co-culturing model to show that mycobacterial ESAT-6 induced neutrophil ROS production and neutrophil necrosis [8]. Necrotic neutrophil debris were then phagocytosed by macrophages, which also underwent necrotic cell death thus promoting the growth of *Mtb*. Inhibition of ROS production by neutrophil myeloperoxidase inhibited necrosis and bacterial growth.

There is also evidence that *Mtb* seeks to inhibit host antioxidant capacity. Human patients show increased levels of systemic oxidative damage, and a reduced systemic antioxidant capacity [9]. Palanisamy *et al*. recapitulated these findings in a guinea pig *Mtb* infection model, and showed that treatment with the oxidant scavenger *N*-acetyl cysteine (NAC), partially ablated the reduced antioxidant capacity and decreased markers of oxidative damage at the site of the lesion [10] . They also showed that NAC-treated animals had fewer necrotic granulomas.

Cyclic nitroxides are low molecular weight stable radicals that have potent antioxidant activity *in vitro* and *in vivo*, and have been cleared for human clinical use [11]. They readily

cross cell membranes, and diffuse into tissues [12, 13]. They afford extensive protection to cells when toxicity is mediated by the production of ROS and RNS [14]. 4-Methoxy-2,2,6,6-tetramethylpiperidine 1-oxyl, shortened to MetT, is a stable cyclic nitroxide derivative based on TEMPO, with a substitution at position 4 for a methoxy group [15]. The complete characterisation of the functional difference of this substitution to other nitroxides is lacking in the literature, but MetT appears to have similar toxicity [16].

Given the serious issues with the current pathogen directed treatment paradigm in TB, and the evidence that host oxidant production is implicated in the progression of *Mtb* infection, there is a basis for investigating cyclic nitroxide antioxidants as host directed therapies for TB. Here we investigate the utility and mechanisms of action of MetT as a model powerful antioxidant therapy for TB using the zebrafish-*M. marinum* infection model. Although the zebrafish-*M. marinum* infection model does not recapitulate the tissue-specific factors involved in human-*Mtb* pulmonary infection, it is a powerful model of natural host-mycobacterial interactions and granuloma biology.

2. Materials and Methods

2.1. Zebrafish husbandry methods.

Adult zebrafish (*Danio rerio*) were maintained at the Garvan Institute Biological Testing Facility and eggs were collected by natural spawning (St Vincent's Hospital AEC Approval 1511). Lines used in this study: TAB strain wild types, *Tg(lyzC:DsRed^{nz50})* [17], *Tg(mfap4:TdTomato^{xt12})* [18], *Tg(mpeg1:tomato-caax^{xt3})* [18], *Durif* mutant in *mpx* gene *(drf^{gl8}) Tg(mpx :EGFP^{i114})* [19, 20]. All experiments and procedures were completed in accordance with Sydney Local Health District Animal Welfare Committee for zebrafish embryo research.

2.2. Microinjection of *Mycobacterium marinum*.

Infection was carried out as previously described [21]. Briefly, 36-48 hour post fertilisation (hpf) embryos were anesthetised in 160 μg/ml tricaine (MS-222, Sigma) and injected with approximately 200 fluorescent *M. marinum* into the venous plexus. Embryos were recovered into fresh zebrafish media (E3 supplemented with phenylthiourea at 45 μg/ml to inhibit pigmentation). Fluorescent *M. marinum* strains were marked by pMSP12 plasmids expressing tdKatushka2 (pTEC22, Addgene 30181), tdTomato (pTEC27, Addgene 30182), Wasabi (pTEC15, Addgene 30174) [22, 23].

2.3. Drug treatments.

Drugs were added directly to zebrafish media immediately after infection unless otherwise indicated. Drugs were replenished every second day for the duration of the experiment. Zebrafish experiments used final concentrations of 1 mM MetT, 3 μM diphenyleneiodonium (DPI) and 50 μg/ml dexamethasone.

2.4. Imaging embryos.

Epifluorescence microscopy was performed using a Leica M205FA fluorescence microscope, Leica DM600B light and fluorescence microscope, or GE Health Care Deltavision Elite inverted fluorescence microscope. Confocal microscopy was performed with a Leica SP5 inverted confocal microscope. Images were processed initially with Leica native LAS software then with ImageJ (NIH).

2.5. Dihydrorhodamine staining.

Biological oxidants were identified *in vivo* with live embryos treated with 500 μM dihydrorhodamine-123 (DHR; Sigma) and incubated for 30 minutes in dark conditions. Embryos were extensively washed prior to imaging.

2.6. Cellrox staining.

Cellular oxidative stress was quantified *in vivo* with live embryos treated with 5 μM Cellrox Far Red (Thermofisher) and incubated for 1 hour in dark conditions [24]. Embryos were extensively washed prior to imaging on a Deltavision Elite (GE Health Care).

2.7. Mitosox staining.

Mitochondrial superoxide was quantified *in vivo* with live embryos treated with 10 μM Mitosox Far Red (Thermofisher) and incubated for 1 hour in dark conditions [24]. Embryos were extensively washed prior to imaging on a Deltavision Elite (GE Health Care). Mitosox Red fluorescence was detected using the mismatched combination of a FITC excitation filter and a TRITC emission filter.

2.6. FRR2 mitochondrial oxidant probe staining.

Mitochondrial ROS was quantified using the flavin-rhodamine redox sensor 2 (FRR2) probe with confocal microscopy [25]. Embryos were treated with 100 μM FRR2 for 2 hours in dark conditions at 28°C, extensively washed and mounted in 1% low melting point agarose for confocal imaging.

Katushka fluorescent protein (expressed by *M. marinum*) was excited in one scan, with a 561 nm laser set to and detector set to 700-800 nm. The mitochondrial probe FFR2 was excited with another scan with the 488 nm argon laser (below significant excitation of bacterial Katushka) and the detector for red emission set to 560-630 nm.

2.7. TUNEL assay.

Cell death was quantified with a Click-iT™ Plus TUNEL Assay for In Situ Apoptosis Detection, Alexa Fluor™ 488 dye kit (ThermoFisher) according to manufacturer's directions. Briefly,

embryos were fixed in 10% v/v neutral buffered formalin (NBF) overnight at 4˚C, washed in PBS then permeabilised by digestion with 10 μg/mL proteinase K for 30 min before post fixing in 10% NBF at 37˚C for 5 min. Embryos were preincubated in Tdt reaction buffer for 10 min at 37˚C then for a further 30 min at 37˚C with Tdt reaction buffer containing Tdt enzyme and EdUTP. Following Tdt reaction embryos were rinsed in PBS and incorporated EdUTP was detected with the Click-iT™ plus TUNEL reaction cocktail for 30 min at 37˚C in the dark, which incorporates Alexa Fluor 488 fluorescent marker to the EdUTP by Click chemistry. Embryos were extensively rinsed in PBS prior to imaging.

2.8. Image processing and analysis.

Infection burden and fluorescent probe staining were measured from images collected by fluorescent microscopy with consistent capture settings as the number of pixels above background per embryo in ImageJ using binary thresholding of single florescence channel images and the Analyze Particles function [23, 26]. Fluorescent probe intensity was measured as the maximum signal using the ImageJ Measure function.

For granuloma-specific measurements: granulomas were traced by eye using bacterial fluorescence as a guide and defined as regions of interest (ROI) in Imagej. Each ROI was then subjected to bacterial fluorescent pixel count to determine bacterial burden in the bacterial fluorescence channel, and the other readout channel was “measured” using Imagej to determine maximum fluorescent pixel intensity, fluorescent pixel count to measure area above a consistent intensity threshold, or manually counted as appropriate.

2.9. Quantitative PCR.

10-40 embryos were pooled and homogenised with a 21-gauge syringe in Trizol reagent (Thermo Fisher Scientific) for total RNA extraction. cDNA was reverse transcribed using the

High-Capacity cDNA Reverse Transcription Kit (Thermo Fisher Scientific). qPCR was carried out using PowerUP SYBR Green Mastermix (Thermo Fisher Scientific) on an Aglient Technologies Mx300P thermal cycler. PCR cycling conditions were 95˚C for 10 minutes, then 40 cycles of 95˚C for 15 seconds and 60 degrees for 1 minute, followed by a melt curve between 55 ˚C and 95 ˚C with 1.5 ˚C/second ramp rate. Primer pairs 5'-3' were: *il1b* ATCAAACCCCAATCCACAGAGT and GGCACTGAAGACACCACGTT, il8 TGTTTTCCTGGCATTTCTGACC and TTTACAGTGTGGGCTTGGAGGG, ef1a TGCCTTCGTCCCAATTTCAG and TACCCTCCTTGCGCTCAATC, tnf GTTTATCAGACAACCGTGGCCA and GATGTTCTCTGTTGGGTTTCTGAC [27].

2.10. Mycobacterial *in vitro* culture and CFU measurements.

M. marinum-TdTomato or *M. marinum Δesx1 pCherry/peredox* was grown in 7H9 Mycobacterial media (Difco Middlebrook), enriched with 10% w/v OADC and 50 µg/mL hygromycin, and cultured at 28°C without agitation with drugs at final concentrations indicated. Samples of the broth culture were serially diluted and plated on 7H10 Mycobacterial agar (Difco). Plates were incubated for at least 7 days at 28°C and CFU were manually counted.

2.11. Hypoxic culture

Bacterial cultures or zebrafish embryos were co-incubated with an Oxoid™ CampyGen™ 2.5 L Sachet (Thermo Fisher Scientific) and maintained in either a 2.5 L (bacterial cultures) or 5 L (zebrafish) airtight container for an expected oxygen concentration of 5% or 10% respectively.

2.12. Statistical analysis

Data are presented as means ± standard deviation. Statistical tests as indicated were carried out in Prism 7 (Graph Pad) using T-tests for experiments with only two groups and ANOVA for multiple comparisons using Tukey post hoc test. Significance is indicated as: $P < 0.05$ *, $P < 0.01$ **, $P < 0.001$ ***.

3. Results

3.1. Macrophages and neutrophils are both prolific producers of oxidants during mycobacterial infection of zebrafish.

We first characterised the time course of host oxidant production during *M. marinum* infection of zebrafish embryos using the fluorescent oxidant probe dihydrorhodamine 123 (DHR). We observed constitutive staining of presumptive lateral line cells throughout the time course with only visible puncta of DHR staining apparent at the 5 dpi time point (Fig 1A). Quantification of granuloma-specific DHR fluorescence intensity from captured images demonstrated a increase in host oxidant production throughout the course of infection (Fig 1B).

To investigate the sources of host oxidant production, macrophage reporter embryos *Tg(mfap4:tdTomato)*^{xt12} and neutrophil reporter embryos *Tg(lyzC:DsRed)*^{nz50} were infected with fluorescent *M. marinum* and stained with DHR.

Fluorescence imaging identified colocalisation of *M. marinum*-Katushka and macrophages in *Tg(mfap4:tdTomato)*^{xt12} embryos (Fig 1C). Many of the infected macrophages also showed of staining with rhodamine, suggesting extensive production of oxidants within macrophages, as anticipated from previous work by Roca and Ramakrishnan [28].

Similarly, fluorescent imaging of *M. marinum*-infected *Tg(lyzC:dsred)*^{nz50} neutrophil reporter embryos revealed colocalisation of *M. marinum*-Katushka and neutrophils, however to a much lesser extent than *M. marinum* and macrophages (Fig 1D). DHR staining suggested little colocalisation of infected *lyzC:dsred* neutrophils and rhodamine indicating a minor contribution of neutrophils to the total production of oxidants at the site of infection.

3.2. The cyclic nitroxide antioxidant 4-methoxyTEMPO decreases mycobacterial burden in the zebrafish embryo.

Next we examined the potential for the cyclic nitroxide antioxidant 4-methoxy-TEMPO (MetT) to inhibit mycobacterial growth and dissemination *in vivo*. Zebrafish embryos were infected with fluorescent *M. marinum*-TdTomato and imaged for bacterial burden at 3 and 5 days post infection (dpi) with drug treatment initiated immediately after infection (Fig 2A and 2B).

A fluorescent pixel count method was used to estimate bacterial burden in these infected embryos (Figure 2C). At 3 dpi, MetT treated embryos had similar bacterial burden compared with untreated infected control embryos. However, at 5 dpi, MetT-treated embryos had significantly less bacterial burden than control embryos.

We next asked if MetT treatment would be active against an established infection by waiting until 4 dpi to start treatment. Analysis of bacterial burden at 5 dpi in this experimental setting again revealed less bacteria in the treated group than in the control group demonstrating a relatively late window of treatment efficacy (Fig 2D), consistent with our relatively late appearance of significant DHR staining during infection (Fig 1B).

3.3. MetT reduces mitochondrial oxidants within the granuloma.

Cyclic nitroxides are known to decrease the accumulation of oxidants in biological environments through multiple mechanisms including direct radical scavenging and through acting as a superoxide dismutatse mimetic [14, 15, 29]. Given that phagosomal oxidants are associated with host protection and mycobacterial killing, we hypothesised that MetT may act on a different component to inhibit bacterial growth *in vivo*. Mitochondrial ROS is upregulated during mycobacterial infection and is associated with host-cell death and the dissemination of the infection [7, 8].

We first attempted to image oxidant production after overnight MetT treatment using DHR staining but observed excessive background fluorescence, possibly caused by a direct reaction between the two reagents. Instead we utilised Cellrox staining of cellular oxidative stress and observed a significant reduction of Cellrox fluorescence intensity in the MetT-treated group consistent with reduced cellular ROS production (Figure 3A).

To test our hypothesis that alleviation of excessive mitochondrial ROS production is a mechanism of action for MetT therapy, we next stained embryos with Mitosox as a mitochondrial superoxide indicator. We observed a significant reduction in Mitosox fluorescence maximal and mean intensity in and around granulomas from the MetT-treated group suggesting reduced mitochondrial ROS production (Figure 3B, 3C, and 3D).

We next visualised mitochondrial ROS using confocal microscopy of zebrafish embryos stained with the flavin-rhodamine redox sensor 2 (FRR2) probe for higher resolution confirmation of our Mitosox data [25]. Oxidised FRR2 exhibits a strong red fluorescence that we could quantify from confocal microscopy. Zebrafish embryos were infected with *M. marinum*-katushka and stained with FRR2 probe at 5 dpi. FRR2 fluorescence extensively localised with areas of *M. marinum,* indicating mitochondrial ROS production at the site of

infection (white arrows in Fig 3D), while the adjacent non-infected tissue did not show evidence of FRR2 fluorescence (Fig 3E).

Quantification of infection-induced FRR2 oxidised from fluorescence above background fluorescence revealed a less red fluorescent FRR2 signal per granuloma in MetT-treated embryos (Fig 3F). Given that the lower bacterial burden of MetT-treated embryos could be expected to correlate with less mitochondrial ROS production, we next calculated the proportional area of FRR2 fluorescence per unit of mycobacteria in each granuloma. Again, MetT-treated embryos had reduced area of oxidised FRR2 probe per unit of mycobacteria per granuloma compared to control embryos that were not treated with MetT (Fig 3G).

3.4. MetT reduces cell death in the mycobacterial granuloma

Having shown that MetT acts to reduce mitochondrial ROS in the granuloma and inhibits the growth of *M. marinum* in the zebrafish embryo we next sought to determine the effect of MetT on cell death in the mycobacterial granuloma. Terminal deoxynucleotidyl transferase dUTP nick end labelling (TUNEL) allows for the *in situ* identification of cells that have undergone necroptotic and apoptotic cell death.

Embryos were infected with *M. marinum*-Katushka, and treated either continuously with MetT or overnight with MetT from late in 4 dpi and were fixed at 5 dpi for TUNEL staining (Fig 4A). Embryos that were continuously treated with MetT had significantly less TUNEL stained cells per granuloma than untreated control embryos (Fig 4B). Additionally, calculating the number of TUNEL stained cells per unit of fluorescent mycobacteria per granuloma revealed a significant reduction in cell death between both MetT treatment groups and the untreated control group (Fig 4C). These correlative data suggest MetT treatment may reduce

immunopathology and bacterial spread by reducing cell death in the mycobacterial granuloma.

3.5. The MetT-induced reduction in bacterial burden is accompanied by an increase in the transcription of inflammatory genes.

MetT has been shown to be potently anti-inflammatory, inhibiting the expression of inflammatory cytokines and reducing leukocyte recruitment to sites of active inflammation [30-32]. Given this documented anti-inflammatory effect we investigated the effect that MetT had on the production of inflammatory genes during mycobacterial infection by quantitative real-time PCR (qPCR) at 5 dpi. Transcription of *tnfa* was unchanged and, surprisingly, there was an increase in the expression of *interleukin 1b*, *interleukin 8*, and *matrix metalloprotease 9* in MetT-treated infected embryos compared to control embryos (Fig 5A).

3.6. Neutrophil myeloperoxidase is dispensable for immunity to *M. marinum* infection in zebrafish.

Our previous work has demonstrated a potent inhibitor effect of MetT on neutrophil myeloperoxidase [32]. To examine the role of myeloperoxidase in mycobacterial infection, zebrafish embryos were raised from a cross of myeloperoxidase heterozygous knockout adults (mpx +/-) and a myeloperoxidase homozygous knockout (mpx -/-) on a transgenic neutrophil reporting *Tg(mpx:EGFP^{i114})* background [19]. These embryos were infected with fluorescent *M. marinum*-TdTomato and imaged for bacterial burden at 3 and 5 dpi.

GFP-expressing *mpx* positive neutrophils were present at sites of *M. marinum* infection both in the early granuloma at 3 dpi and at the late granuloma at 5 dpi regardless of functional Mpx state (Fig 5B). There was no gross difference in the pattern of infection, with similar dissemination of the bacteria and size of individual granulomas (Fig 5C). Furthermore,

myeloperoxidase knockout animals had similar bacterial burden to their heterozygous clutchmates at 3 and 5 dpi (Fig 5D).

3.7. MetT exerts immunopathology-independent effects on *M. marinum in vivo*.

To test our hypothesis that MetT reduces host immunopathology, we next examined the effect MetT in the context of infection by *ΔESX1* mutant *M. marinum* that are deficient in the major mycobacterial granuloma-driving pathogenicity factor [33]. MetT reduced the *ΔESX1* mutant *M. marinum* burden (Fig 5E). However, we noted that the magnitude of the MetT-induced reduction on the *ΔESX1* mutants burden was much smaller than seen for infections with the parental *M. marinum*, approximately 40% reduction in mutants compared to 90% reduction in parental strain infections suggesting that multiple mechanisms of action, one of which is countering ESX1-driven immunopathology.

Complementary to this investigation, we suppressed host immunity using dexamethasone. Dexamethasone treatment significantly increased mycobacterial burden as bacteria grew largely uncontained by granulomas. MetT treatment was still effective in the dexamethasone immunosuppressed background but was unable to return bacterial burden to the level of immunocompetent embryos treated with MetT (Fig 5F). Together these data demonstrate the existence of immune dependent and independent mechanisms of action for MetT against mycobacterial infection.

3.8. MetT does not inhibit *M. marinum* growth *in vitro* under standard growth conditions.

Recent literature has described a direct antimicrobial effect of the NOX and NOS inhibitor diphenyleneiodonium (DPI). Next we determined whether MetT had a similar direct inhibitory effect on *M. marinum* growth that would account for the zebrafish infection phenotypes. Thus, axenic cultures of freshly diluted *M. marinum* cultures were supplemented

with MetT at final concentrations of 1 and 5 mM, and colony forming units (CFUs) per mL of culture media were measured. Overall, no significant differences in bacterial CFUs were observed (Fig 6A).

3.9. MetT can disrupt NADH:NAD+ balance in *M. marinum*.

Given our observation that MetT affects eukaryotic mitochondrial ROS production, we reasoned MetT may also affect mycobacterial energetics. To visualise disruption of cellular respiration in *M. marinum*, we created a transgenic *M. marinum Δesx1* strain carrying pMV762-Peredox-mCherry (Addgene 90217) to visualise build up of NADH:NAD ratio [34, 35]. Analysis of constitutive mCherry expression in a late log culture revealed a small but statistically significant decrease in bacteria number following 1 mM MetT treatment and a larger decrease following 5 mM MetT treatment that was correlated with CFU counts (Fig 6B).

Calculation of the ratio of peredox:mCherry fluorescence revealed that 5 mM MetT treatment modestly increased the NADH:NAD ratio, suggesting a mechanism of antibacterial action via electron transport chain disruption, similar to that seen for bedaquiline treatment, in late growth phases *in vitro* (Figure 6C).

3.10. Hypoxic stress sensitises *M. marinum* to MetT *in vitro* and *in vivo*.

Hypoxic mycobacteria are more sensitive to electron transport chain disruption and we have previously demonstrated the presence of hypoxia in the zebrafish embryo-*M. marinum* infection model [36-38]. To better model the growth-restrictive conditions found in the *in vivo* infection microenvironment, we next asked if hypoxia could sensitise *M. marinum* to inhibition by MetT *in vitro*. Comparison of recovered CFUs revealed that culture in 5% atmospheric oxygen sensitised *M. marinum* to killing by 5 mM MetT (Fig 6D).

This finding suggested we would be able to increase the *in vivo* sensitivity of *M. marinum* by incubating infected embryos in reduced oxygen conditions. We incubated infected embryos in approximately 10% atmospheric oxygen, which did not affect embryo morphology (Fig 6E). We treated embryos with a shortened suboptimal course of MetT to only 4 dpi, prior to any significant effect on burden, to facilitate identification of an interaction between hypoxia and MetT. We observed an additive effect of hypoxia and MetT treatment *in vivo* (Fig 6F).

4. Discussion

We have demonstrated MetT-mediated inhibition of *M. marinum* infection *in vivo* in the zebrafish embryo model, and identified beneficial host- and bacterial-directed effects of MetT treatment. We present a range of live and *in situ* imaging data linking MetT treatment to reduced pathological mitochondrial ROS production and cell death during late mycobacterial infection. Furthermore, stressors found *in vivo* sensitised *M. marinum* to growth restriction or killing by MetT in axenic culture.

The development of multi-drug resistant and extensively drug resistant *Mtb* has shown that the current treatment regimen for tuberculosis is susceptible to evasion and resistance. Traditional pathogen-directed therapies, such as antibiotics, are susceptible to drug resistance caused by spontaneous mutations that are driven by the selective pressure of antibiotic exposure [39]. As host-directed therapies do not directly target bacterial proteins, theoretically there is a reduced risk of drug resistance [40]. However, while there is the reduced risk of drug resistance there is concurrently an increased risk of side-effects since host biology is targeted [41]. While a systematic examination of the toxicity of MetT was beyond the scope of the current study, MetT did not appear to induce an observable pathological phenotype at efficacious doses.

Neutrophils were also examined as a potential target for MetT as they are present at the site of mycobacterial infection and are producers of ROS. Neutrophils primarily kill bacteria through myeloperoxidase, an enzyme that produces potently microbicidal hypochlorous acid and could trigger macrophage necrosis during infection [8, 42]. Recently, MetT was identified as a potent inhibitor of myeloperoxidase-induced production of hypochlorous acid in an *in vitro* neutrophil co-culture model of acute myocardial infarction [32]. However, using a loss of function mutant of neutrophil myeloperoxidase we show that myeloperoxidase is dispensable for control of mycobacterial infection by zebrafish embryos. This finding complements a study by Yang et al. demonstrating that neutrophils have a host protective role in early mycobacterial infection through a NOX dependant pathway and the extensive literature that describes neutrophils having an undefined, but probably limited role in the control of *Mtb* infection [43].

The vast majority of mitochondrial ROS is superoxide generated from the mitochondrial electron transport chain [44]. Cyclic nitroxide derivatives such as MetT have documented superoxide dismutase mimetic effects whereby they reduce superoxide radicals to oxygen and water. It is by this mechanism that we hypothesise MetT reduces mitochondrial oxidants during mycobacterial infection [14, 45, 46]. However, FRR2 is a non-specific oxidant probe, which is fluorescent when oxidised by many reactive oxygen species and nitrogen species. Similarly, there are well-documented limitations to the commercially available stains that we have utilised in our study namely; the nonspecific nature of DHR fluorescence in response to a multitude of oxidant species, and the overlapping fluorescent spectra of specifically and non-specifically oxidised Mito-SOX fluorescence [47, 48]. Future studies could dissect the precise targets of MetT responsible for the reduction in granuloma ROS *in vivo*.

Cell death modality is crucial to the pathogenesis of mycobacterial infection [49]. Caspase dependent apoptosis has been demonstrated to be important in the control of mycobacterial infection [50-52]. Pathogenic mycobacteria deploy virulence factors such as ESX1 to supress macrophage apoptosis, further suggesting the host protective effects of apoptosis [33]. Conversely necroptosis, a more inflammatory cell death, fuels disease [7, 53]. Given that MetT induces a concurrent reduction in mitochondrial oxidants, cell death and bacterial burden, and that apoptosis is likely host protective, it is an attractive hypothesis that MetT is selectively inhibiting mitochondrial ROS dependant necroptosis. While we demonstrate an inhibition of cell death through TUNEL (see Figure 3.6), TUNEL cannot differentiate between apoptosis and necroptosis [54]. More detailed investigations of cell death are required to determine whether MetT is indeed acting selectively on necroptotic pathways, or rather than as a bulk inhibitor of cell death resulting in the same net effect.

Our finding of an increase in the expression of *interleukin 1b*, *interleukin 8*, and *matrix metalloprotease 9* despite reduced mycobacterial burden in MetT-treated embryos was surprising as these inflammatory genes are usually thought to correlate with mycobacterial burden. We interpret the inverse correlation between inflammatory gene expression and bacterial burden following MetT treatment as evidence of better immune control of infection due to immune cell survival within the granuloma. Combined with our finding that MetT is efficacious in an immunosuppressed dexamethasone background, our data adds evidence for important role of net granuloma macrophage survival in the successful containment of mycobacterial infection [28]. Interestingly, a recent paper studying the zebrafish immune response to uric acid crystals placed *il1b* transcription downstream of mitochondrial ROS production potentially demonstrating an important divergence in the immune activation pathways in the context of different chronic stressors [55].

MetT does not inhibit the growth of mycobacteria during the early stages of infection or *in vitro* culture. Instead, inhibition of bacterial growth only becomes apparent around 5 dpi. By 3 dpi, infected macrophages have migrated into deep tissues and have formed tight granuloma aggregations [56]. Between 3 and 5 dpi, there is a dramatic expansion of bacterial load and macrophage cell death. Macrophage depletion around this stage exacerbates necroptosis, and promotes bacterial growth [57]. Our findings support this narrative by MetT-mediated interception of pro-necroptotic ROS production to aid immune containment of infection. From the bacterial perspective, the later timepoint correlates to a much more hostile environment correlating with increased sensitivity to MetT-mediated electron transport chain disruption.

In conclusion, the cyclic nitroxide antioxidant MetT acts on the host and bacterium to inhibit the growth and dissemination of mycobacterial infection in a zebrafish model of tuberculosis. MetT inhibits mitochondrial ROS production and cell death at the site of infection sparing tissue. More broadly, the data presented here demonstrate the value of performing drug discovery in complex model systems to detect *in vivo* microenvironment-drug target interactions.

Acknowledgements

Dr Kristina Jahn and Sydney Cytometry for assistance with imaging equipment; Garvan Biological Testing Facility staff, Ms Jennifer Brand, Mr Michael Pickering, Ms Rola Bazzi, Dr Lucie Nedved and Dr Stephanie Allison, at the Garvan Institute of Medical Research for maintenance of zebrafish breeding stock; Professor Graham Lieschke for supplying the *durif* mutant line. The authors thank Mr Joshua “Yeezy” Kasparian and Dr Matt Johansen for helpful discussions and technical assistance.

This work was supported by the Australian National Health and Medical Research Council grants APP1099912 and APP1053407; The University of Sydney Fellowship G197581; NSW Ministry of Health under the NSW Health Early-Mid Career Fellowships Scheme H18/31086; and the Kenyon Family Inflammation Award (S.H.O.).

Author contributions: H.B., P.K.W., B.C., and S.H.O. designed the experiments. H.B., W.X., E.H., and S.H.O performed the experiments. S.R. generated the *M. marinum* peredox reporter strain. E.J.N. generated experimental fluorescent redox probes. H.B. and S.O. wrote the paper. W.J.B., P.K.W., B.C., and S.H.O. supervised the project.

References

[1] World Health Organization., Global Tuberculosis Programme., Global tuberculosis control : WHO report, Global Tuberculosis Programme, Geneva, p. 15 volumes.
[2] A. O'Garra, P.S. Redford, F.W. McNab, C.I. Bloom, R.J. Wilkinson, M.P. Berry, The immune response in tuberculosis, Annual review of immunology 31 (2013) 475-527.
[3] J.D. MacMicking, Cell-autonomous effector mechanisms against mycobacterium tuberculosis, Cold Spring Harbor perspectives in medicine 4(10) (2014).
[4] C.J. Cambier, K.K. Takaki, R.P. Larson, R.E. Hernandez, D.M. Tobin, K.B. Urdahl, C.L. Cosma, L. Ramakrishnan, Mycobacteria manipulate macrophage recruitment through coordinated use of membrane lipids, Nature 505(7482) (2014) 218-222.
[5] D. Salvemini, H. Ischiropoulos, S. Cuzzocrea, Roles of nitric oxide and superoxide in inflammation, Inflammation Protocols (2003) 291-303.
[6] A.M. Pisoschi, A. Pop, The role of antioxidants in the chemistry of oxidative stress: A review, Eur J Med Chem 97 (2015) 55-74.
[7] F.J. Roca, L. Ramakrishnan, TNF dually mediates resistance and susceptibility to mycobacteria via mitochondrial reactive oxygen species, Cell 153(3) (2013) 521-534.
[8] T. Dallenga, U. Repnik, B. Corleis, J. Eich, R. Reimer, G.W. Griffiths, U.E. Schaible, M. tuberculosis-Induced Necrosis of Infected Neutrophils Promotes Bacterial Growth Following Phagocytosis by Macrophages, Cell Host & Microbe 22(4) (2017) 519-530.e3.
[9] S. Kwiatkowska, G. Piasecka, M. Zieba, W. Piotrowski, D. Nowak, Increased serum concentrations of conjugated diens and malondialdehyde in patients with pulmonary tuberculosis, Respiratory medicine 93(4) (1999) 272-276.
[10] G.S. Palanisamy, N.M. Kirk, D.F. Ackart, C.A. Shanley, I.M. Orme, R.J. Basaraba, Evidence for oxidative stress and defective antioxidant response in guinea pigs with tuberculosis, Plos one 6(10) (2011) e26254.
[11] B.P. Soule, F. Hyodo, K.-i. Matsumoto, N.L. Simone, J.A. Cook, M.C. Krishna, J.B. Mitchell, Therapeutic and clinical applications of nitroxide compounds, Antioxidants & redox signaling 9(10) (2007) 1731-1744.
[12] Y. Kinoshita, K.-i. Yamada, T. Yamasaki, F. Mito, M. Yamato, N. Kosem, H. Deguchi, C. Shirahama, Y. Ito, K. Kitagawa, N. Okukado, K. Sakai, H. Utsumi, In vivo evaluation of novel

nitroxyl radicals with reduction stability, Free Radical Biology and Medicine 49(11) (2010) 1703-1709.
[13] H.V.T. Nguyen, Q. Chen, J.T. Paletta, P. Harvey, Y. Jiang, H. Zhang, M.D. Boska, M.F. Ottaviani, A. Jasanoff, A. Rajca, J.A. Johnson, Nitroxide-Based Macromolecular Contrast Agents with Unprecedented Transverse Relaxivity and Stability for Magnetic Resonance Imaging of Tumors, ACS Central Science 3(7) (2017) 800-811.
[14] J.B. Mitchell, W. DeGraff, D. Kaufman, M.C. Krishna, A. Samuni, E. Finkelstein, M.S. Ahn, S.M. Hahn, J. Gamson, A. Russo, Inhibition of oxygen-dependent radiation-induced damage by the nitroxide superoxide dismutase mimic, tempol, Archives of biochemistry and biophysics 289(1) (1991) 62-70.
[15] D. Metodiewa, A. Kochman, J. Skolimowski, L. Gebicka, C. Koska, Metexyl (4-methoxy-2,2,6,6-tetramethylpiperidine-1-oxyl) as an oxygen radicals scavenger and apoptosis inducer in vivo, Anticancer research 19(6b) (1999) 5259-64.
[16] Z. Zhang, Z. Ren, S. Chen, X. Guo, F. Liu, L. Guo, N. Mei, ROS generation and JNK activation contribute to 4-methoxy-TEMPO-induced cytotoxicity, autophagy, and DNA damage in HepG2 cells, Archives of Toxicology (2017).
[17] C. Hall, M.V. Flores, T. Storm, K. Crosier, P. Crosier, The zebrafish lysozyme C promoter drives myeloid-specific expression in transgenic fish, BMC Dev Biol 7(1) (2007) 42.
[18] E.M. Walton, M.R. Cronan, R.W. Beerman, D.M. Tobin, The Macrophage-Specific Promoter mfap4 Allows Live, Long-Term Analysis of Macrophage Behavior during Mycobacterial Infection in Zebrafish, PLoS ONE 10(10) (2015) e0138949.
[19] L. Pase, J.E. Layton, C. Wittmann, F. Ellett, C.J. Nowell, C.C. Reyes-Aldasoro, S. Varma, K.L. Rogers, C.J. Hall, M.C. Keightley, P.S. Crosier, C. Grabher, J.K. Heath, S.A. Renshaw, G.J. Lieschke, Neutrophil-delivered myeloperoxidase dampens the hydrogen peroxide burst after tissue wounding in zebrafish, Curr Biol 22(19) (2012) 1818-24.
[20] S.A. Renshaw, C.A. Loynes, D.M.I. Trushell, S. Elworthy, P.W. Ingham, M.K.B. Whyte, A transgenic zebrafish model of neutrophilic inflammation, Blood 108(13) (2006) 3976-3978.
[21] M.A. Matty, S.H. Oehlers, D.M. Tobin, Live Imaging of Host-Pathogen Interactions in Zebrafish Larvae, Methods Mol Biol 1451 (2016) 207-23.
[22] K. Takaki, C.L. Cosma, M.A. Troll, L. Ramakrishnan, An in vivo platform for rapid high-throughput antitubercular drug discovery, Cell reports 2(1) (2012) 175-84.
[23] K. Takaki, J.M. Davis, K. Winglee, L. Ramakrishnan, Evaluation of the pathogenesis and treatment of Mycobacterium marinum infection in zebrafish, Nat Protoc 8(6) (2013) 1114-24.
[24] V. Mugoni, A. Camporeale, M.M. Santoro, Analysis of oxidative stress in zebrafish embryos, J Vis Exp (89) (2014).
[25] A. Kaur, K. Jankowska, C. Pilgrim, S.T. Fraser, E.J. New, Studies of Hematopoietic Cell Differentiation with a Ratiometric and Reversible Sensor of Mitochondrial Reactive Oxygen Species, Antioxid Redox Signal 24(13) (2016) 667-79.
[26] E.M. Walton, M.R. Cronan, C.J. Cambier, A. Rossi, M. Marass, M.D. Foglia, W.J. Brewer, K.D. Poss, D.Y.R. Stainier, C.R. Bertozzi, D.M. Tobin, Cyclopropane Modification of Trehalose Dimycolate Drives Granuloma Angiogenesis and Mycobacterial Growth through Vegf Signaling, Cell Host Microbe 24(4) (2018) 514-525 e6.
[27] S.H. Oehlers, M.V. Flores, C.J. Hall, R. O'Toole, S. Swift, K.E. Crosier, P.S. Crosier, Expression of zebrafish cxcl8 (interleukin-8) and its receptors during development and in response to immune stimulation, Dev Comp Immunol 34(3) (2010) 352-9.
[28] F.J. Roca, L. Ramakrishnan, TNF Dually Mediates Resistance and Susceptibility to Mycobacteria via Mitochondrial Reactive Oxygen Species, Cell 153(3) (2013) 521-34.
[29] O. Augusto, D.F. Trindade, E. Linares, S.M. Vaz, Cyclic nitroxides inhibit the toxicity of nitric oxide-derived oxidants: mechanisms and implications, Anais da Academia Brasileira de Ciências 80(1) (2008) 179-189.

[30] S. Neil, J. Huh, V. Baronas, X. Li, H.F. McFarland, M. Cherukuri, J.B. Mitchell, J.A. Quandt, Oral administration of the nitroxide radical TEMPOL exhibits immunomodulatory and therapeutic properties in multiple sclerosis models, Brain Behav Immun 62 (2017) 332-343.
[31] R.F. Queiroz, A.K. Jordao, A.C. Cunha, V.F. Ferreira, M.R. Brigagao, A. Malvezzi, A.T. Amaral, O. Augusto, Nitroxides attenuate carrageenan-induced inflammation in rat paws by reducing neutrophil infiltration and the resulting myeloperoxidase-mediated damage, Free Radic Biol Med 53(10) (2012) 1942-53.
[32] B. Chami, G. Jeong, A. Varda, A.M. Maw, H.B. Kim, G.M. Fong, M. Simone, B.S. Rayner, X.S. Wang, J.M. Dennis, P.K. Witting, The nitroxide 4-methoxy TEMPO inhibits neutrophil-stimulated kinase activation in H9c2 cardiomyocytes, Arch Biochem Biophys 629 (2017) 19-35.
[33] H.E. Volkman, H. Clay, D. Beery, J.C. Chang, D.R. Sherman, L. Ramakrishnan, Tuberculous granuloma formation is enhanced by a mycobacterium virulence determinant, PLoS Biol 2(11) (2004) e367.
[34] S.A. Bhat, I.K. Iqbal, A. Kumar, Imaging the NADH:NAD(+) Homeostasis for Understanding the Metabolic Response of Mycobacterium to Physiologically Relevant Stresses, Front Cell Infect Microbiol 6 (2016) 145.
[35] Y.P. Hung, J.G. Albeck, M. Tantama, G. Yellen, Imaging cytosolic NADH-NAD(+) redox state with a genetically encoded fluorescent biosensor, Cell Metab 14(4) (2011) 545-54.
[36] S.H. Oehlers, M.R. Cronan, N.R. Scott, M.I. Thomas, K.S. Okuda, E.M. Walton, R.W. Beerman, P.S. Crosier, D.M. Tobin, Interception of host angiogenic signalling limits mycobacterial growth, Nature 517(7536) (2015) 612-5.
[37] S.P. Rao, S. Alonso, L. Rand, T. Dick, K. Pethe, The protonmotive force is required for maintaining ATP homeostasis and viability of hypoxic, nonreplicating Mycobacterium tuberculosis, Proc Natl Acad Sci U S A 105(33) (2008) 11945-50.
[38] K. Hards, J.R. Robson, M. Berney, L. Shaw, D. Bald, A. Koul, K. Andries, G.M. Cook, Bactericidal mode of action of bedaquiline, The Journal of antimicrobial chemotherapy 70(7) (2015) 2028-37.
[39] J.E. Gomez, B.B. Kaufmann-Malaga, C.N. Wivagg, P.B. Kim, M.R. Silvis, N. Renedo, T.R. Ioerger, R. Ahmad, J. Livny, S. Fishbein, J.C. Sacchettini, S.A. Carr, D.T. Hung, Ribosomal mutations promote the evolution of antibiotic resistance in a multidrug environment, Elife 6 (2017).
[40] A. Schwegmann, F. Brombacher, Host-Directed Drug Targeting of Factors Hijacked by Pathogens, Science Signaling 1(29) (2008) re8-re8.
[41] D.M. Tobin, Host-Directed Therapies for Tuberculosis, Cold Spring Harbor perspectives in medicine 5(10) (2015).
[42] Y. Kato, Neutrophil myeloperoxidase and its substrates: formation of specific markers and reactive compounds during inflammation, J Clin Biochem Nutr 58(2) (2016) 99-104.
[43] C.T. Yang, C.J. Cambier, J.M. Davis, C.J. Hall, P.S. Crosier, L. Ramakrishnan, Neutrophils exert protection in the early tuberculous granuloma by oxidative killing of mycobacteria phagocytosed from infected macrophages, Cell Host Microbe 12(3) (2012) 301-12.
[44] D. Han, M.D. Ybanez, S. Ahmadi, K. Yeh, N. Kaplowitz, Redox regulation of tumor necrosis factor signaling, Antioxid Redox Signal 11(9) (2009) 2245-63.
[45] A. Dhanasekaran, S. Kotamraju, C. Karunakaran, S.V. Kalivendi, S. Thomas, J. Joseph, B. Kalyanaraman, Mitochondria superoxide dismutase mimetic inhibits peroxide-induced oxidative damage and apoptosis: role of mitochondrial superoxide, Free Radical Biology and Medicine 39(5) (2005) 567-583.
[46] J.B. Mitchell, A. Samuni, M.C. Krishna, W.G. DeGraff, M.S. Ahn, U. Samuni, A. Russo, Biologically active metal-independent superoxide dismutase mimics, Biochemistry 29(11) (1990) 2802-2807.

[47] B. Kalyanaraman, V. Darley-Usmar, K.J. Davies, P.A. Dennery, H.J. Forman, M.B. Grisham, G.E. Mann, K. Moore, L.J. Roberts, 2nd, H. Ischiropoulos, Measuring reactive oxygen and nitrogen species with fluorescent probes: challenges and limitations, Free Radic Biol Med 52(1) (2012) 1-6.
[48] J. Zielonka, B. Kalyanaraman, Hydroethidine- and MitoSOX-derived red fluorescence is not a reliable indicator of intracellular superoxide formation: another inconvenient truth, Free Radic Biol Med 48(8) (2010) 983-1001.
[49] A.H. Moraco, H. Kornfeld, Cell death and autophagy in tuberculosis, Seminars in immunology 26(6) (2014) 497-511.
[50] R.E. Butler, P. Brodin, J. Jang, M.S. Jang, B.D. Robertson, B. Gicquel, G.R. Stewart, The balance of apoptotic and necrotic cell death in Mycobacterium tuberculosis infected macrophages is not dependent on bacterial virulence, PLoS One 7(10) (2012) e47573.
[51] F. Winau, S. Weber, S. Sad, J. de Diego, S.L. Hoops, B. Breiden, K. Sandhoff, V. Brinkmann, S.H. Kaufmann, U.E. Schaible, Apoptotic vesicles crossprime CD8 T cells and protect against tuberculosis, Immunity 24(1) (2006) 105-17.
[52] P. Espinosa-Cueto, A. Magallanes-Puebla, C. Castellanos, R. Mancilla, Dendritic cells that phagocytose apoptotic macrophages loaded with mycobacterial antigens activate CD8 T cells via cross-presentation, PLoS One 12(8) (2017) e0182126.
[53] C. Fleury, B. Mignotte, J.L. Vayssiere, Mitochondrial reactive oxygen species in cell death signaling, Biochimie 84(2-3) (2002) 131-41.
[54] B. Grasl-Kraupp, B. Ruttkay-Nedecky, H. Koudelka, K. Bukowska, W. Bursch, R. Schulte-Hermann, In situ detection of fragmented DNA (tunel assay) fails to discriminate among apoptosis, necrosis, and autolytic cell death: A cautionary note, Hepatology 21(5) (1995) 1465-1468.
[55] C.J. Hall, L.E. Sanderson, L.M. Lawrence, B. Pool, M. van der Kroef, E. Ashimbayeva, D. Britto, J.L. Harper, G.J. Lieschke, J.W. Astin, K.E. Crosier, N. Dalbeth, P.S. Crosier, Blocking fatty acid-fueled mROS production within macrophages alleviates acute gouty inflammation, J Clin Invest 128(5) (2018) 1752-1771.
[56] J.M. Davis, H. Clay, J.L. Lewis, N. Ghori, P. Herbomel, L. Ramakrishnan, Real-Time Visualization of Mycobacterium-Macrophage Interactions Leading to Initiation of Granuloma Formation in Zebrafish Embryos, Immunity 17(6) (2002) 693-702.
[57] A.J. Pagán, C.-T. Yang, J. Cameron, L.E. Swaim, F. Ellett, G.J. Lieschke, L. Ramakrishnan, Myeloid growth factors promote resistance to mycobacterial infection by curtailing granuloma necrosis through macrophage replenishment, Cell host & microbe 18(1) (2015) 15-26.

Figure Legends

Figure 1: Macrophages and neutrophils produce ROS during mycobacterial infection in zebrafish.

(A) Representative images of DHR-stained ROS production (green) from 1, 3, and 5 dpi zebrafish embryos overlayed with *M. marinum*-tomato fluorescence (red). Arrows in 5 dpi panels indicate granulomas with visible DHR puncta. Scale bars indicate 1 mm.

(B) Quantification of DHR-stained ROS production by maximum pixel intensity measurement around the area defined by bacterial fluorescence from individual granulomas in *M. marinum*-infected zebrafish embryos. n=10 embryos per timepoint, each dot indicates a measurement from single granuloma from the tail region of an infected embryo.

(C) Representative images of DHR-stained ROS production (green) by *mfap4*-expressing macrophages (red) in a 5 dpi zebrafish embryo infected with *M. marinum*-katushka (magenta). Image on right shows overlay of only DHR-stained ROS production (green) and *mfap4*-expressing macrophages (red) highlighting ROS production by infected macrophages in the granuloma. Frame is of a single granuloma in the caudal haematopoietic tissue region of the embryo. Scale bar indicates 100 μm.

(D) Representative images of DHR-stained ROS production (green) by *lyzC*-expressing neutrophils (red) in a 5 dpi zebrafish embryo infected with *M. marinum*-katushka (magenta). Image on right shows overlay of only DHR-stained ROS production (green) and *lyzC*-expressing neutrophils highlighting a lower proportion ROS production by neutrophils (red). Frame is of a single granuloma in the caudal haematopoietic tissue region of the embryo, diffuse green signal on the left of the frame is yolk staining. Scale bar indicates 100 μm.

Figure 2: MetT treatment reduces mycobacterial burden *in vivo*

(A) Representative images of 3 dpi zebrafish embryos infected with *M. marinum*-tomato and treated with MetT. Arrowheads indicate site of primary infection.

(B) Representative images of 5 dpi zebrafish embryos infected with *M. marinum*-tomato and treated with MetT. Arrowheads indicate site of primary infection.

(C) Quantification of bacterial burden by fluorescent pixel count in 3 and 5 dpi zebrafish embryos treated with MetT. Bacterial fluorescence area data for all groups are expressed relative to the mean value for 5 dpi control group.

(D) Quantification of bacterial burden by fluorescent pixel count in 5 dpi zebrafish embryos treated overnight with MetT at 4 dpi. Bacterial fluorescence area data are expressed relative to the mean value for the control group.

Each dot in C and D represents one embryo, data is pooled from 3 biological replicates.

Figure 3: MetT treatment reduces mitochondrial ROS production in mycobacterial granulomas.

(A) Quantification of cellular ROS production in granulomas from 5 dpi zebrafish embryos stained with Cellrox. Data is presented as a ratio of maximum Cellrox fluorescence divided by bacterial burden per granuloma. n=10 embryos per group.

(B) Representative images of 5 dpi zebrafish embryos infected with *M. marinum*-cerulean (cyan) and treated with MetT as indicated. Embryos are stained with Mitosox Red (red) for mitochondrial ROS production in granulomas visible by contrast light microscopy. Scale bars indicate 50 μm.

(C) Quantification of mitochondrial superoxide production in granulomas from 5 dpi zebrafish embryos stained with Mitosox. Data is presented as a ratio of maximum Mitosox fluorescence around each granuloma divided by bacterial burden per granuloma. n=10 embryos per group.

(D) Quantification of mitochondrial superoxide production in granulomas from 5 dpi zebrafish embryos stained with Mitosox. Data is presented as a ratio of mean Mitosox fluorescence around each granuloma divided by bacterial burden per granuloma. n=10 embryos per group.

(E) Representative images of 5 dpi zebrafish embryos infected with *M. marinum*-katushka (blue) and treated with MetT as indicated. Embryos are stained with FRR2 (red, and purple colocalisation with blue bacteria) for mitochondrial ROS production in infected cells, indicated by arrows. Scale bars indicate 100 μm.

(F) Quantification of mitochondrial ROS production by granulomas in 5 dpi zebrafish embryos stained with FRR2. Area of FFR2 fluorescence above background is measured around each granuloma. n=5 embryos per group.

(G) Quantification of mitochondrial ROS production by granulomas in 5 dpi zebrafish embryos stained with FRR2. Relative intensity is calculated as a ratio of maximum FFR2 fluorescence divided by bacterial burden per granuloma. n=5 embryos per group.

Figure 4: MetT treatment reduces cell death in mycobacterial granulomas.

(A) Representative images of TUNEL staining for apoptotic and necroptotic cells in granulomas from the CHT region of 5 dpi zebrafish embryos infected with *M. marinum*-katushka and treated with MetT as indicated. Scale bar indicates 100 μm.

(B) Quantification of total TUNEL stained cells per granuloma in 5 dpi zebrafish embryos infected with *M. marinum*-katushka and treated with MetT as indicated. n=20 embryos per group.

(C) Quantification of TUNEL stained cell number divided by the bacterial fluorescence area per granuloma in 5 dpi zebrafish embryos treated with MetT as indicated. n=20 embryos per group.

Figure 5: Effects of MetT treatment on innate immune system.

(A) qPCR quantification of proinflammatory gene expression in 5 dpi zebrafish embryos infected with *M. marinum* and treated with MetT. Genes are *interleukin-1b (il1b), interleukin-8 (il8), matrix metalloprotease 9 (mmp9)* and *tumour necrosis factor a (tnfa)*.

(B) Representative image of neutrophil recruitment to granulomas in 5 dpi durif/mpx homozygous mutants infected with *M. marinum*-tomato. White arrowheads indicate granulomas with *mpx* expressing neutrophil recruitment. Scale bar indicates 1 mm.

(C) Representative images of 5 dpi zebrafish *durif* mutant embryos infected with *M. marinum*-tomato.

(D) Quantification of bacterial burden by fluorescent pixel count in 5 dpi zebrafish *durif* mutant embryos. Bacterial fluorescence area data are expressed relative to the mean value for the heterozygous genotype group.

(E) Quantification of bacterial burden by fluorescent pixel count in 5 dpi zebrafish embryos infected with *ΔESX1* mutant *M. marinum* and treated with MetT as indicated.

(F) Quantification of bacterial burden by fluorescent pixel count in 5 dpi zebrafish embryos treated MetT and dexamethasone as indicated.

D-F each dot represents one embryo.

Figure 6: MetT has antibacterial effects against stressed bacteria.

(A) CFU recovery from axenic early log phase cultures of *M. marinum* treated with MetT for 2 days.

(B) Quantification of constitutive mCherry fluorescence in late log phase cultures of *M. marinum Δesx1* strain carrying pMV762-Peredox-mCherry treated with MetT.

(C) Quantification of peredox fluorescence in late log phase cultures of *M. marinum Δesx1* strain carrying pMV762-Peredox-mCherry treated with MetT as an indicator of cellular NADH:NAD build up.

(D) CFU recovery from early log phase cultures of *M. marinum* treated with MetT for 2 days

(E) Representative images of 4 dpi zebrafish embryos infected with *M. marinum*-wasabi and exposed to 10% O_2 in a hypoxia chamber.

(F) Quantification of bacterial burden by fluorescent pixel count in 4 dpi zebrafish embryos treated MetT and maintained in 10% O_2 as indicated. Each dot represents one embryo.

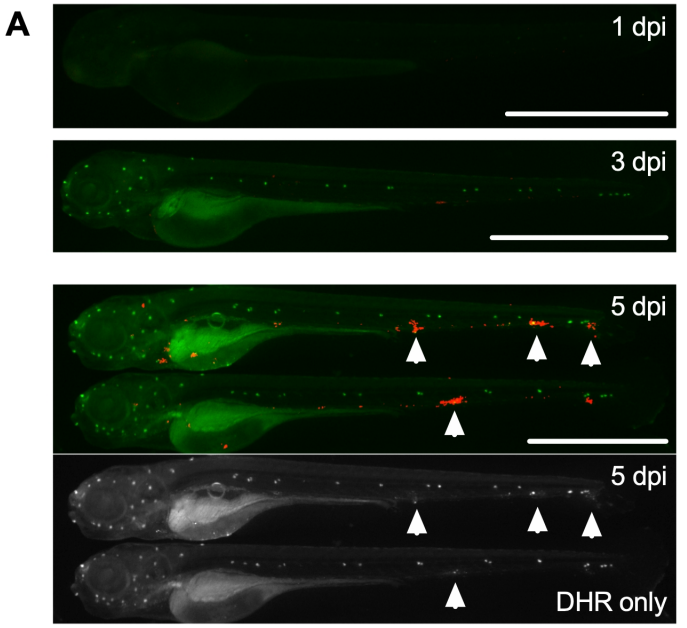
A
1 dpi
3 dpi
5 dpi
5 dpi
DHR only

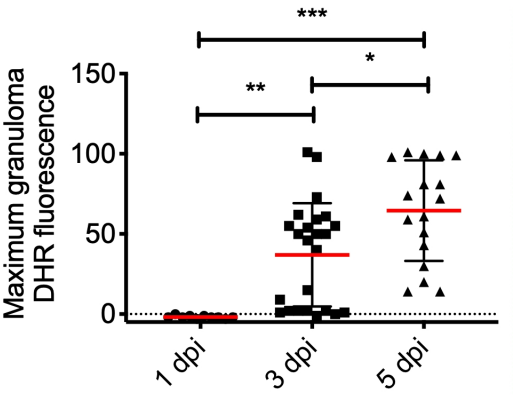
B
***
*
**
Maximum granuloma DHR fluorescence
150
100
50
0
1 dpi
3 dpi
5 dpi

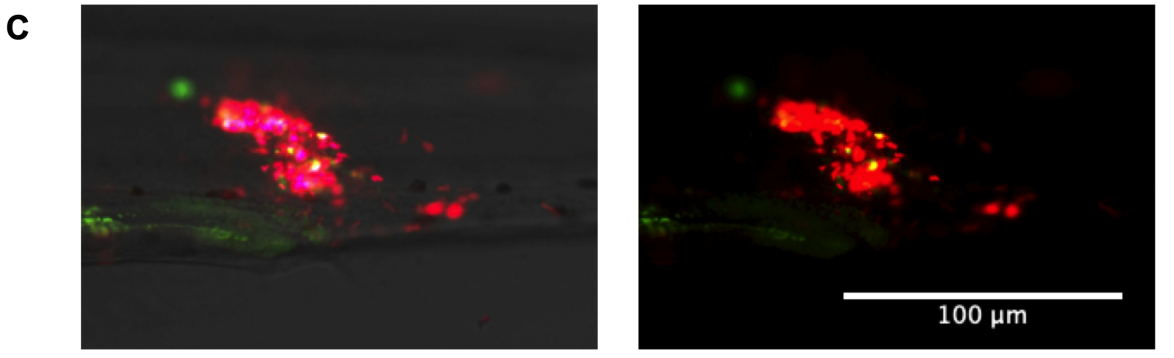
C
100 µm

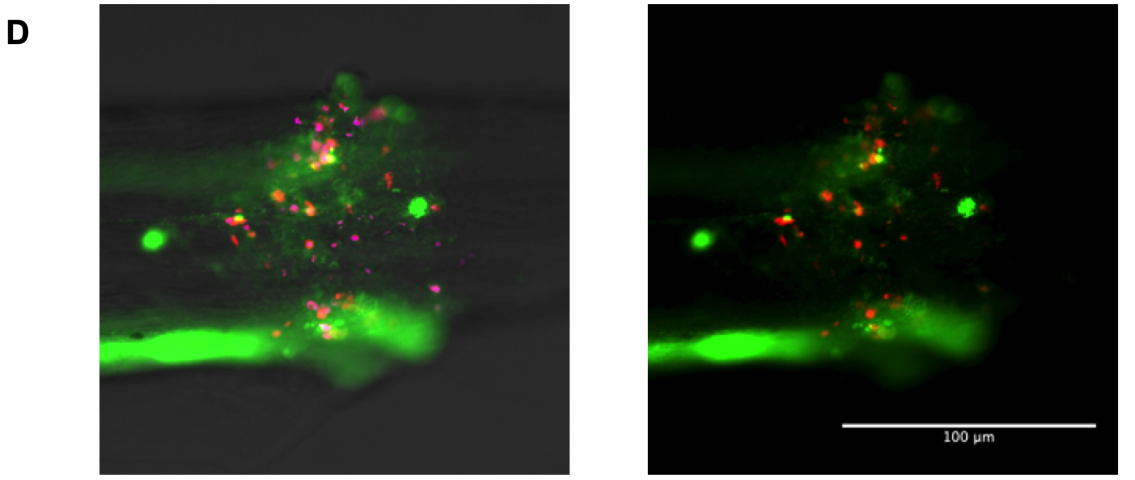
D
100 µm

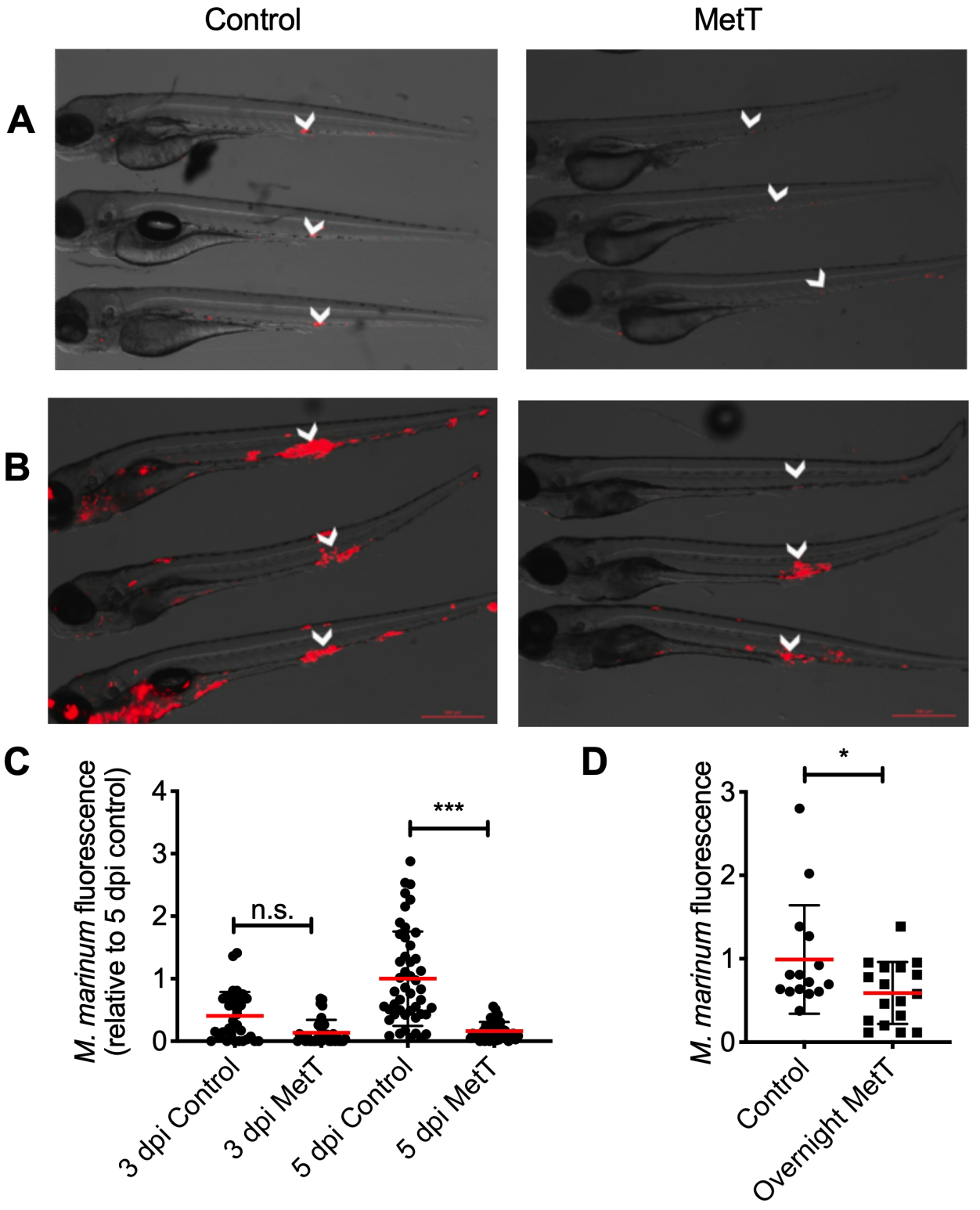
Control
MetT
A
B
C
M. marinum fluorescence (relative to 5 dpi control)
n.s.
***
3 dpi Control
3 dpi MetT
5 dpi Control
5 dpi MetT
D
M. marinum fluorescence
*
Control
Overnight MetT

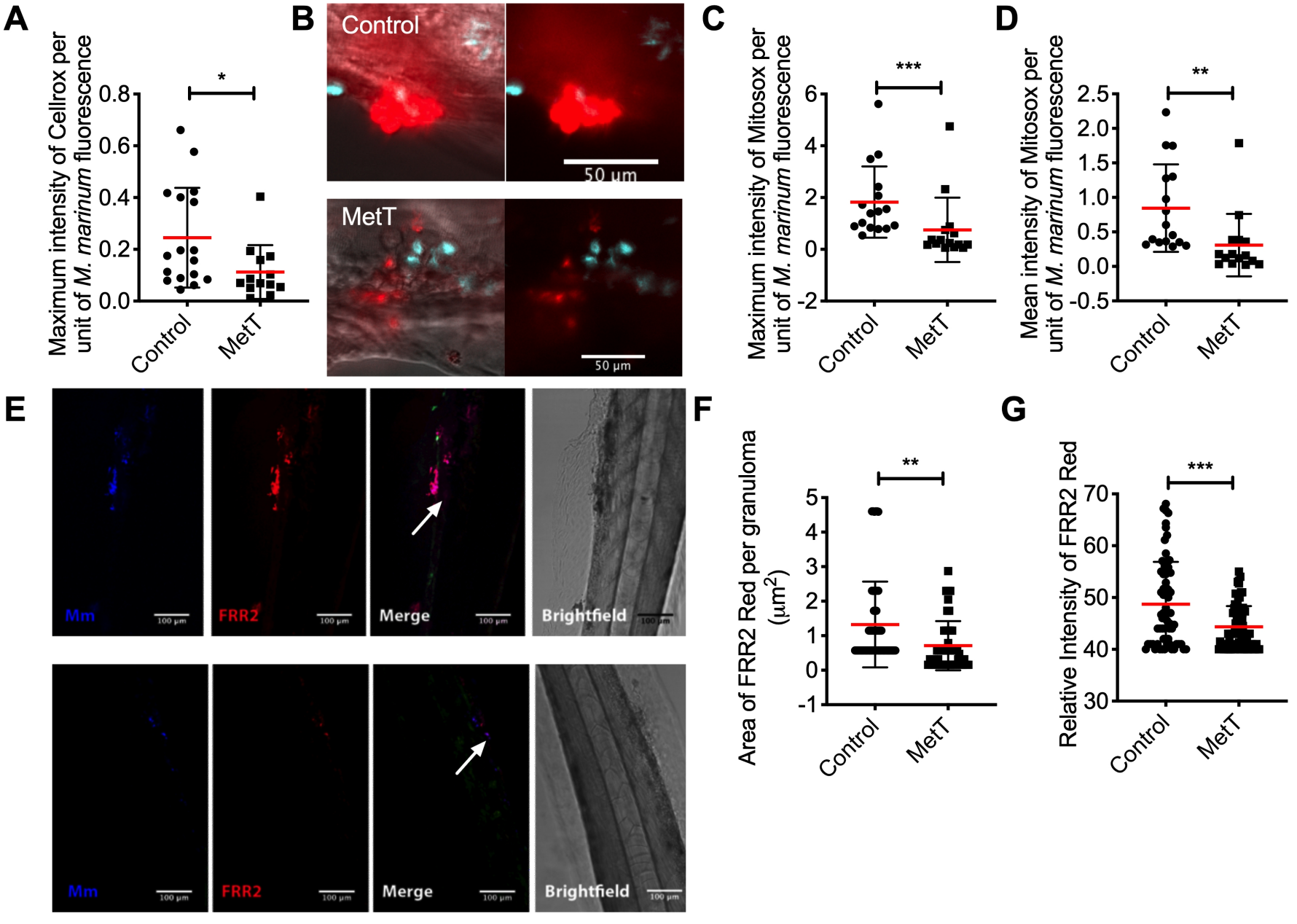
A
Maximum intensity of Cellrox per unit of M. marinum fluorescence
0.8
0.6
0.4
0.2
0.0
*
Control
MetT
B
Control
50 µm
MetT
50 µm
C
Maximum intensity of Mitosox per unit of M. marinum fluorescence
6
4
2
0
-2
***
Control
MetT
D
Mean intensity of Mitosox per unit of M. marinum fluorescence
2.5
2.0
1.5
1.0
0.5
0.0
-0.5
**
Control
MetT
E
Mm
FRR2
Merge
Brightfield
100 µm
F
Area of FRR2 Red per granuloma (µm²)
5
4
3
2
1
0
-1
**
Control
MetT
G
Relative Intensity of FRR2 Red
70
60
50
40
30
***
Control
MetT

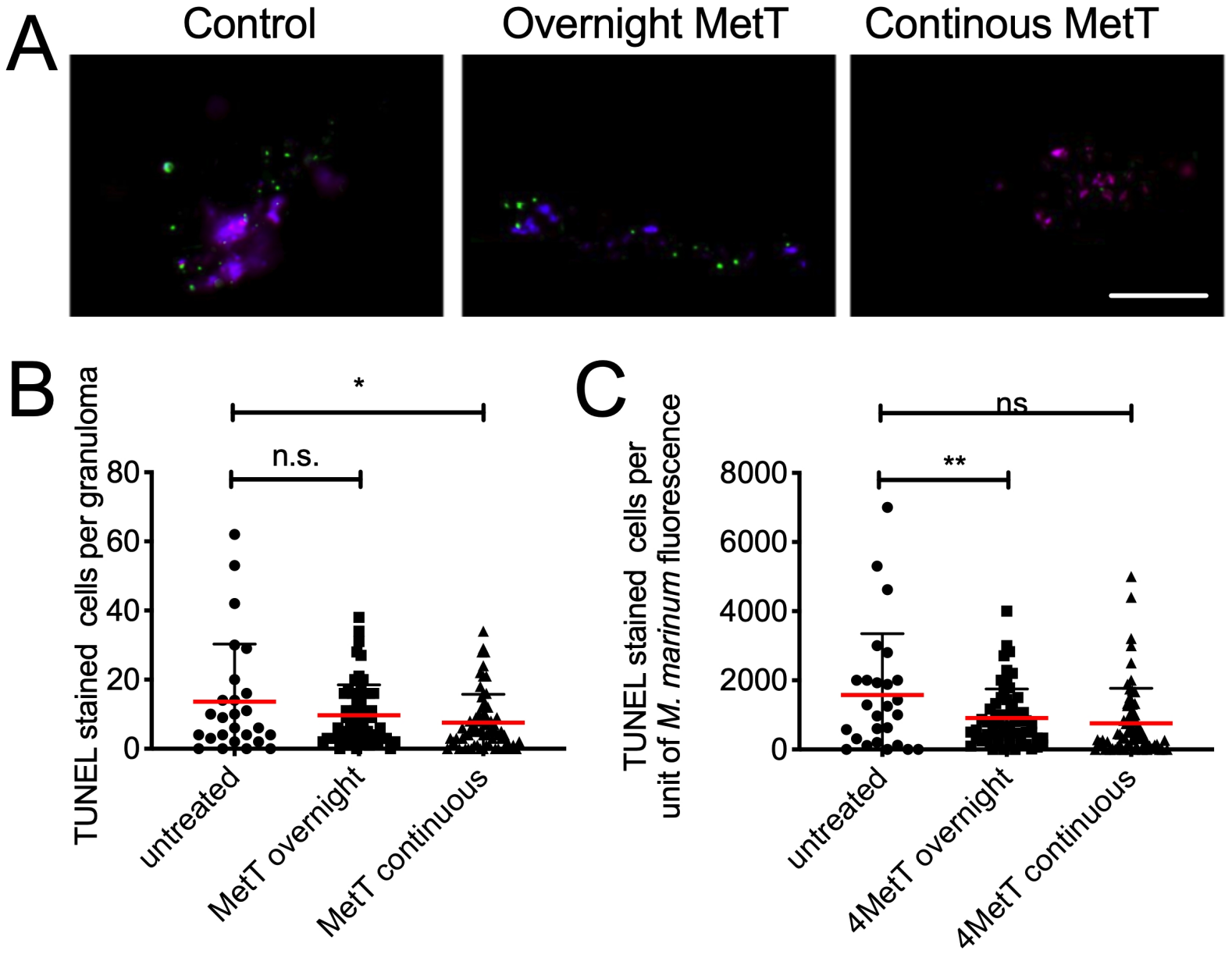
A
Control
Overnight MetT
Continous MetT
B
TUNEL stained cells per granuloma
*
n.s.
80
60
40
20
0
untreated
MetT overnight
MetT continuous
C
TUNEL stained cells per unit of M. marinum fluorescence
ns
**
8000
6000
4000
2000
0
untreated
4MetT overnight
4MetT continuous

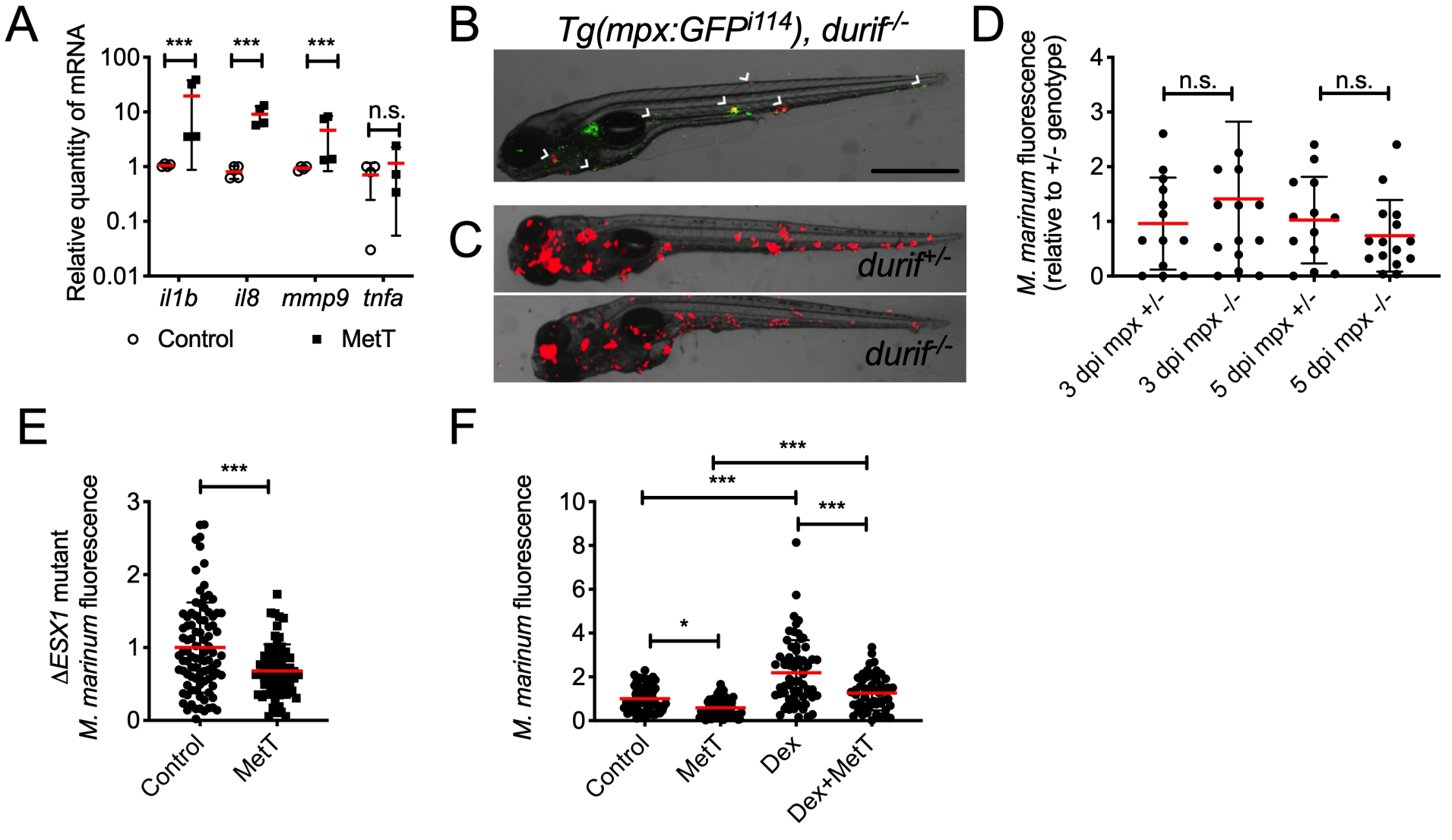
A
Relative quantity of mRNA
100
10
1
0.1
0.01
***
***
***
n.s.
il1b
il8
mmp9
tnfa
Control
MetT
B
Tg(mpx:GFPi114), durif-/-
C
durif+/-
durif-/-
D
M. marinum fluorescence
(relative to +/- genotype)
4
3
2
1
0
n.s.
n.s.
3 dpi mpx +/-
3 dpi mpx -/-
5 dpi mpx +/-
5 dpi mpx -/-
E
ΔESX1 mutant
M. marinum fluorescence
3
2
1
0
***
Control
MetT
F
M. marinum fluorescence
10
8
6
4
2
0
***
***
***
*
Control
MetT
Dex
Dex+MetT

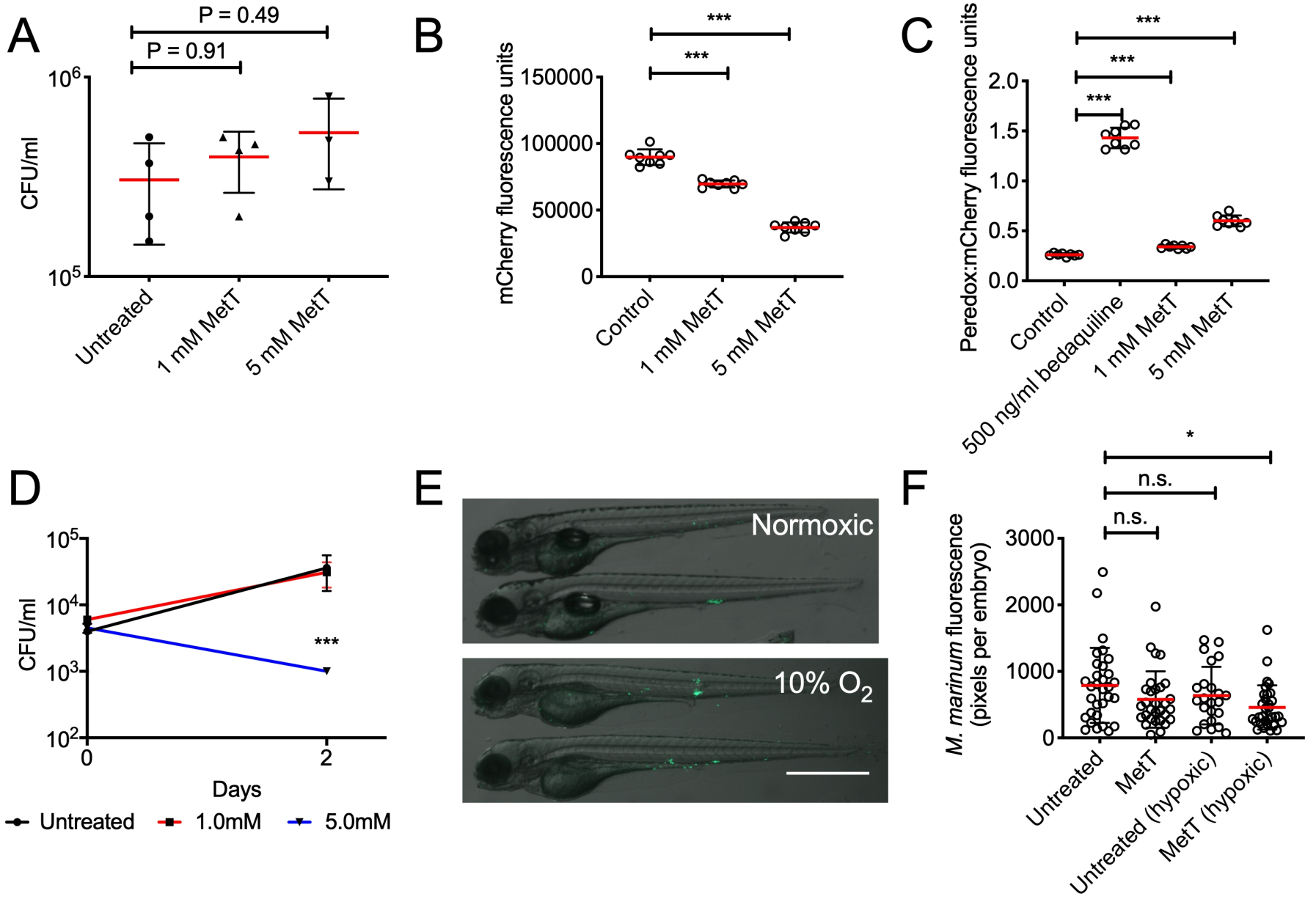
A
P = 0.49
P = 0.91
CFU/ml
Untreated
1 mM MetT
5 mM MetT
B
mCherry fluorescence units
Control
1 mM MetT
5 mM MetT
C
Peredox:mCherry fluorescence units
Control
500 ng/ml bedaquiline
1 mM MetT
5 mM MetT
D
CFU/ml
Days
Untreated
1.0mM
5.0mM
E
Normoxic
10% O2
F
M. marinum fluorescence (pixels per embryo)
n.s.
n.s.
Untreated
MetT
Untreated (hypoxic)
MetT (hypoxic)